

Longterm Late-Wood ^{13}C signatures in Iberian *Pinus pinaster* Ait. induced by climate

W. Lara^{a,c,1,*}, C. Ordoñez^a, F. Bravo^a, C. A. Sierra^a

^aSustainable Forest Management Research Institute, UVA-INIA, Avenida Madrid, s/n,
34071, Palencia, Spain

^bDepartment of Biogeochemical Processes, Max Planck Institute for Biogeochemistry,
Hans-Knöll-Straße 10, 07745, Jena, Germany

^cResearch Center on Ecosystems and Global Change, Carbono & Bosques (C&B), Calle
51A, No 72-23, Int: 601, 050034, Medellín, Colombia

Abstract

Keywords:

¹ **1. Introduction**

² This study aims to study long-term effects of drought on tree growth and
³ isotopic discrimination of *P. pinaster* in north and east-central Spain.

*Corresponding author

¹E-mail address: wilson.lara@alumnos.uva.es (W.Lara)

⁴ This is the introduction

5 **2. Materials and Methods**

6 *2.1. Study area*

7 We developed our study in two areas in east Spain and north-central Spain
8 (Fig. 2). The areas belong to the most vast native provenance region of mar-
9 itime pine (*Pinus pinaster* Ait.) forests, growing on sandy soils (Inceptisols and
10 Aridisols) forming large continuous populations at moderate densities (average
11 of 500 - 1000 trees per hectare). Forest ecosystems of the area are associated
12 with oaks (*Quercus ilex* L., *Q. faginea* Lam., and *Q. pyrenaica* Willd.), beeches
13 (*Fagus silvatica* L.), and other pine species (*Pinus sylvestris* L., *P. nigra* Arn.
14 and *P. halepensis* Mill). Average altitude for this region ranges from 900 m to
15 1000 m above sea level. The forests are influenced by Mediterranean climate
16 with dry and warm summers and cool to mild winters. Mean annual tempera-
17 ture is about 11 °C and mean annual precipitation is approx. 562 mm.

18 *2.2. Core sampling*

19 Dominant trees of maritime pine growing in ten locations in the study site
20 where core sampled (5 mm diameter) at chest height (1.3 m). These were
21 located in five locations of north-central edge of the study site and the other
22 five locations were established on the eastern edge. Two dominant trees were
23 sampled by site, and two core samples were extracted from each tree. The core
24 samples were air dried, sanded, and scanned (1000:1600 ppi). Tree-ring Widths
25 (TRWs) in the scanned images were measured and statistically controlled with
26 R-packages `measuRing` (Lara et al., 2015) and `dplR` (Bunn, 2010), respectively.

27 A master chronology of 150 trees of *P. pinaster* for the study area (Bogino
28 and Bravo, 2008) was used to develop the statistical control of the TRW. The
29 chronology has strong common signal (EPS > 0.95, SNR > 22). The cross-
30 dating process was controlled by grouping the data in four common regions,
31 which were defined after clustering the tree-dimensional coordinates of the sam-
32 pling locations, with each of the clusters having sites at most 80 km of closeness
33 (Figure 1).

34 *2.3. climatic data*

35 We processed a high-resolution gridded dataset (0.11° resol.) of monthly
36 cummulative precipitations and monthly mean temperatures for peninsular Spain
37 (Herrera et al., 2015, Spain02) across Ebro basin (1971 - 2010). Proyection of
38 UTM coordinates of the sample plots to coordinate system in climate algorithm
39 was developed with R-package `rgdal` (Bivand et al., 2015). After projecting the
40 gridded dataset, meteorological series corresponding to coordinates of sample lo-
41 cations were extracted. These were used to compute **Standardized Precipitation**
42 **Indexes (SPI)** extracted with R-packages `raster` (Hijmans, 2015) and `SPI`.

43 *2.4. Late-Wood Stable $\delta^{13}\text{C}$*

44 Analysis of **Late-Wood Stable $\delta^{13}\text{C}$ (LWSC)** were established in one core
45 replicate by sampling location along the study site. Late wood in radial incre-
46 ments of the cores were carefully separated from the earlywood with a micro-
47 tome. Only rings that were formed after 1974 were analysed. Whole wood was
48 milled, an aliquot of 100 mg was packed in porous bags and used for cellulose
49 extraction. The samples were washed in 5 percent NaOH solution twice for 2
50 h at 60°C in order to remove fats, oils, resins and hemicellulose. In a second
51 step the lignin was removed with NaClO 2.7% After each treatment the samples
52 were washed with distilled water and then finally dried overnight at 60°C .

53 The $\delta^{13}\text{C}$ was determined using an elemental analyser linked to an isotopic
54 ratio mass spectrometer via a variable open split interface (Max Plank Institute
55 for Biogeochemistry, Germany). The results of laboratory were presented in the
56 δ notation:

$$\delta = [(R_{sample}/R_{standard}) - 1] \times 10^3 \quad (1)$$

57 relative to the internationsl VPDB standard for cabon; where R_{sample} and
58 $R_{standard}$ is the fractions of $^{13}\text{C}/^{12}\text{C}$ for the sample and the standard, respec-
59 tively. The standard deviation for the repeated analysis (commercial cellulose)
60 was better than 0.1. was better than 0.1 percent. The calibration versus VPDB

61 was done by measuring IAEA USGS-24(graphite) and IAEA-CH7 (polyethylene).
62

63 *2.5. bi*

64 **3. Results**

65 *3.1. Tree-growth fluctuations*

66 Patterns in **TRW** fluctuations were more regular in locations of east Spain
67 than in locations of north-central Spain regardless trends in **TRW** chronologies
68 were or were not subtracted.

69 In locations of east Spain, smoothing spline over time of original **TRW**
70 chronology exhibited regular sinusoidal patterns (Fig. 3, lower-left panel).
71 Lower extremes of the spline were observed during the decade starting in 1990
72 and higher extremes of the spline were evidenced during the decades starting in
73 1970 and 2010. The smooting spline over time in the detrended **TRW** chronol-
74 ogy illustrated similar sinusoidal patterns with regard to the patterns observed
75 in the original **TRW** chronology (Fig. 3, lower-right panel).

76 In locations of north-central Spain, the smooting spline over time of original
77 **TRW** chronology indicated a decreasing exponential pattern (Fig. 3, upper-left
78 panel). Higher extremes of this curve were evidenced in the decade starting in
79 1979 and lower extremes were observed in the decade starting in 2010. The
80 spline of the corresponding detrended chronology was sinusoidal with higher
81 extremes observed in the decades of 1970 and 2000, and the lower extremes
82 observed in the decades starting in 1990 (Fig. 3, upper-right panel).

83 *3.2. Late-Wood Stable $\delta^{13}\text{C}$ fluctuations*

84 In contrast to the tree-growth fluctuations, patterns in **Late-Wood Stable**
85 $\delta^{13}\text{C}$ (**LWSC**) fluctuations were more regular in detrended chronologies than in
86 original chronologies regardless the ubication of the sampling locations.

87 In locations of east Spain, the spline over time in original **LWSC** chronology
88 followed an irregular and decreasing sinusoidal pattern (Fig. 4, lower-left panel)

89 with the maximum extreme of the spline being evidenced during the decade
90 starting in 1980, followed by a pulse with minimum and maximum relatives
91 occurring during the decade of 1990, and ending with lower extremes in the
92 decade starting in 2010. Spline of corresponding detrended LWSC chronology
93 (Fig. 4, lower-right panel) indicated more regular sinusoidal pattern to that
94 observed in the original chronology. This curve had decadal pulses with maximal
95 extremes occurring around 1980, 1990, and 2005.

96 In locations of north Spain, the spline of the original LWSC chronology de-
97 picted irregular and decreasing sinusoidal pattern (Fig. 4, upper-left panel)
98 with spline oscillations slowing during second half of 1980 and a minimum ex-
99 treme occurring around 2005. Spline of detrended LWSC chronology illustrated
100 more regular sinusoidal pattern regard the curve of original chronology (Fig. 4,
101 upper-right panel) with similar slowing oscillation around second half of 1980
102 and minimal relatives occurring around 1975, 1995, and 2010.

103 *3.3. Intra-annual response coefficients*

104 Responses of TRW to monthly climatic fluctuations were similar in both
105 north-central Spain and east Spain (Fig. 5). The tree-growth chronology was
106 correlated with precipitation regimes of the winter season and uncorrelated with
107 precipitations of the other seasons. The significant correlations between tree
108 growth and winter precipitation were slightly stronger in eastern than in north-
109 central edges of study site and occurred within a month of each other: i.e.
110 January in north-central Spain and February in the west. No conclusive rela-
111 tionships between tree growth and seasonal temperature were observed along the
112 study site.

113 On the other hand, responses of LWSC to the monthly fluctuations were dif-
114 ferent in the locations. In north central Spain, the LWSC significantly responded
115 to summer temperatures and no significant correlations were evidenced between
116 the stable isotope and the temperature in the other seasons. No conclusive re-
117 lationships responses between LWSC and temperature were evidenced. In east
118 Spain, the LWSC significantly responded to spring precipitations while no sig-

119 nificant responses were observed in other seasons. No conclusive relationships
120 betwee tree growth and seasonal temperatures were observed along the study
121 site.

122 *3.4. Wavelet coherency*

123 Relationships between tree growth and drought fluctuations depended on
124 sampling locations (Fig. 6). The tree-growth fluctuations in north-central Spain
125 were more responsive to high-frequency fluctuations of drought occurring during
126 last 15 years of the ananlysis. On the other hand, the tree-growth fluctuations of
127 east Spain were responsive to middle-to-low frequency fluctuations that occurred
128 during the all recorded years.

129 In north-central Spain, the **TRW-SPI** cross-spectrum indicated that main
130 correlations in the two time series was in the 2-4 period bands (Fig. 6). The
131 relationship

132 In north-central Spain, cross-coherences between **TRW** and **SPI** were higher
133 in low-to-middle-period fluctuations occurring principally after 1998 (Fig. 6,
134 upper-contour plot).

135 In east Spain, **TRW** and **SPI** cross-choherences were higher in high-period
136 fluctuations along the recorded years (Fig. 6, lower-contour plot) and in low-
137 to-middle-period fluctuations occurring after 1995.

138 **4. References**

139 Bivand, R., Keitt, T., Rowlingson, B., 2015. rgdal: Bindings for the Geospatial
140 Data Abstraction Library. URL: <https://CRAN.R-project.org/package=rgdal>. r package version 1.1-1.

142 Bogino, S.M., Bravo, F., 2008. Growth response of *Pinus pinaster* ait.
143 to climatic variables in central spanish forests. Ann. For. Sci. 65, 1–13.
144 doi:[10.1051/forest:2008025](https://doi.org/10.1051/forest:2008025).

145 Bunn, A.G., 2010. Statistical and visual crossdating in r using the dplr library.
146 Dendrochronologia 28, 251 – 258. doi:[10.1016/j.dendro.2009.12.001](https://doi.org/10.1016/j.dendro.2009.12.001).

147 Herrera, S., Fernández, J., Gutiérrez, J., 2015. Update of the Spain02 gridded
148 observational dataset for EURO-CORDEX evaluation: assessing the effect of
149 the interpolation methodology. International Journal of Climatology .

150 Hijmans, R.J., 2015. raster: Geographic data analysis and modeling. URL:
151 <https://CRAN.R-project.org/package=raster>. r package version 2.4-30.

152 Lara, W., Bravo, F., Sierra, C., 2015. measuRing: An R package to measure
153 tree-ring widths from scanned images. Dendrochronologia 34, 43 – 50. doi:[10.1016/j.dendro.2015.04.002](https://doi.org/10.1016/j.dendro.2015.04.002).

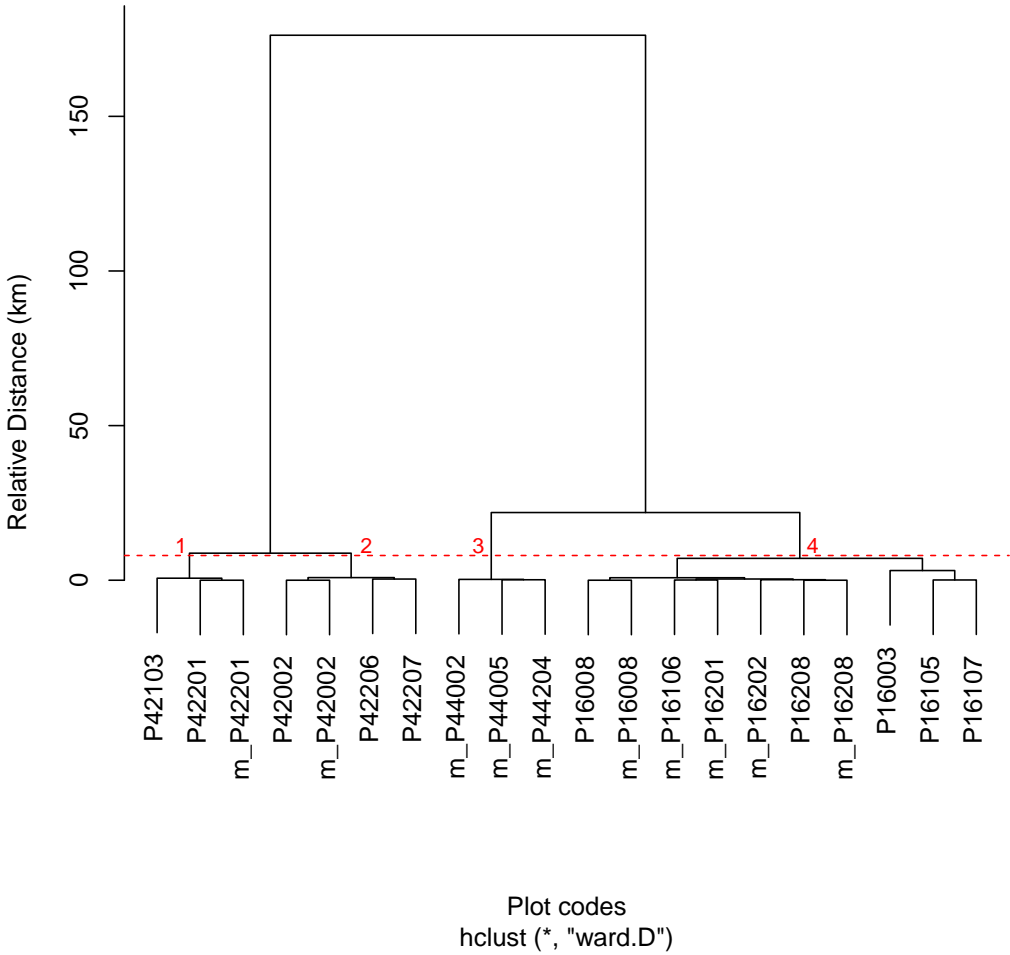


Figure 1: Geographic closeness among Tree-ring Width (TRW) chronologies of *Pinus Pinaster* Ait. (*P. pinaster*). Master chronologies are indicated with m_. Codes of the chronologies begin with initial letter of the species. The following two digits in the codes indicate spanish provinces: 42 (*Soria*) and 44 (*teruel*) in north-central Spain, and 16 (*Cuenca*) in eastern Spain. The last three digits in the codes are plot labels. Red dashed line and red numbers define four within-group cross-dating chronologies (< 8 km of cossenes)

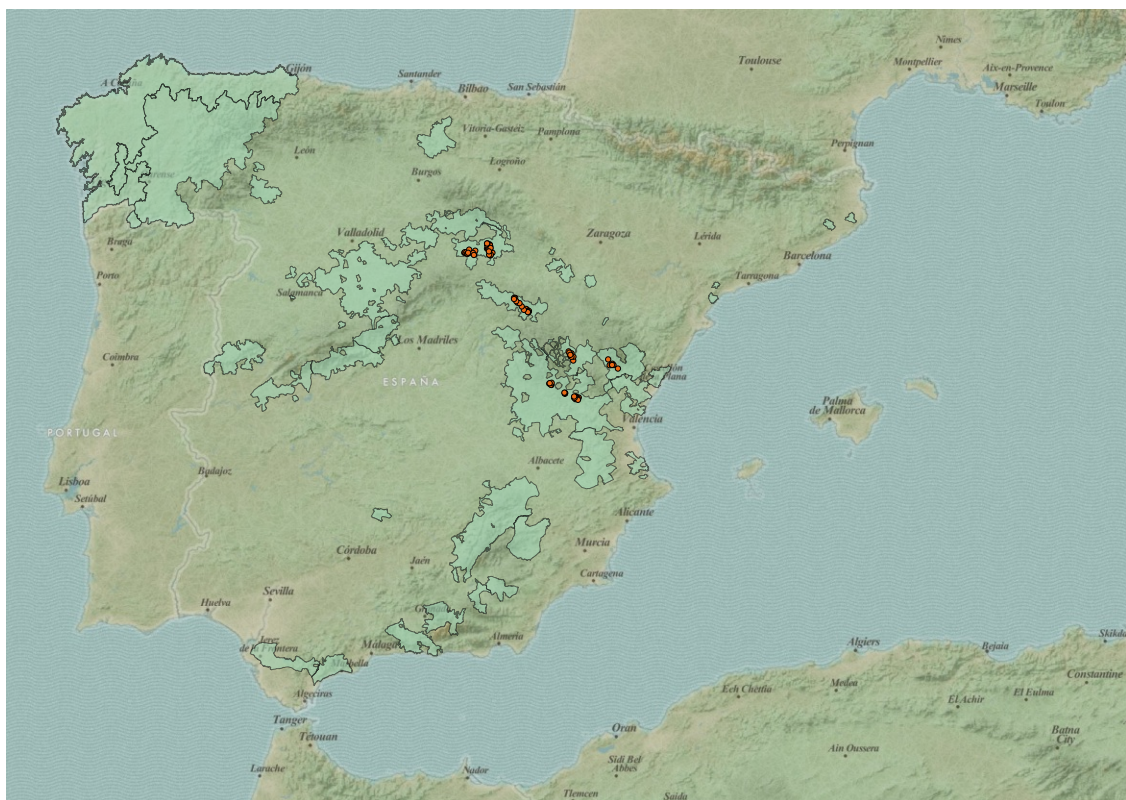


Figure 2: Study site. The green areas represent distribution of *P. pinaster* trees along Spain. The orange points represent locations of tree-ring chronologies.

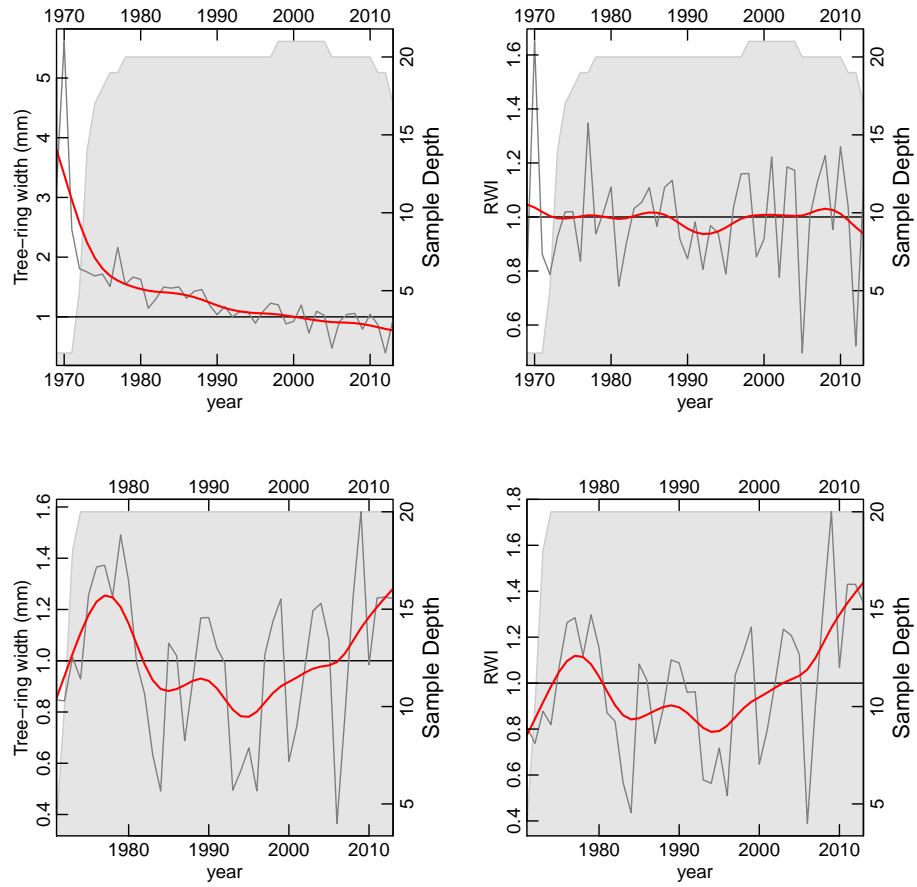


Figure 3: TRW chronologies of *P. pinaster* trees in north-central Spain (upper-panel plots) and eastern Spain (lower-panel plots). Original chronologies (left-panel plots) are detrended (right-panel plots). Gray lines are the fluctuations, and red lines (smoothing splines) are average patterns. Sample depth is the number of series available in each year.

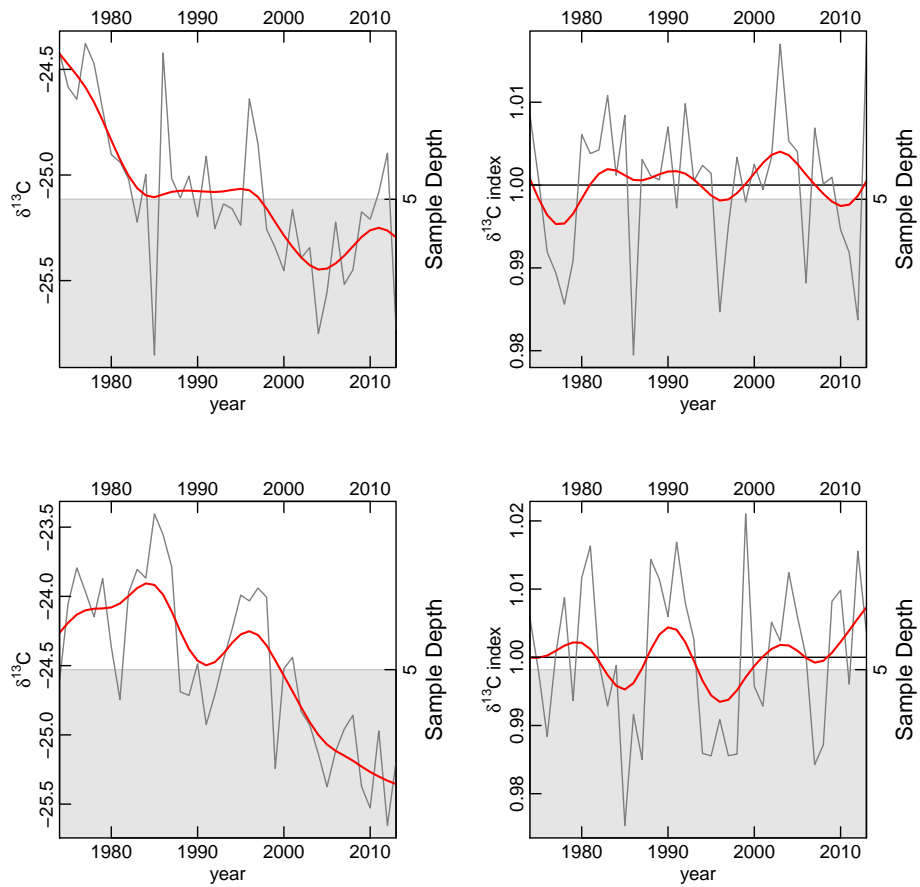


Figure 4: Late-Wood Stable $\delta^{13}\text{C}$ chronologies of *P. pinaster* trees growing on north-central Spain (upper-panel plots) and eastern Spain (lower-panel plots). Trends in the original chronologies (left-panel plots) are subtracted (right-panel plots). Gray lines are fluctuations and red lines (smoothing splines) are average patterns. Sample depth is the number of series available in each year.

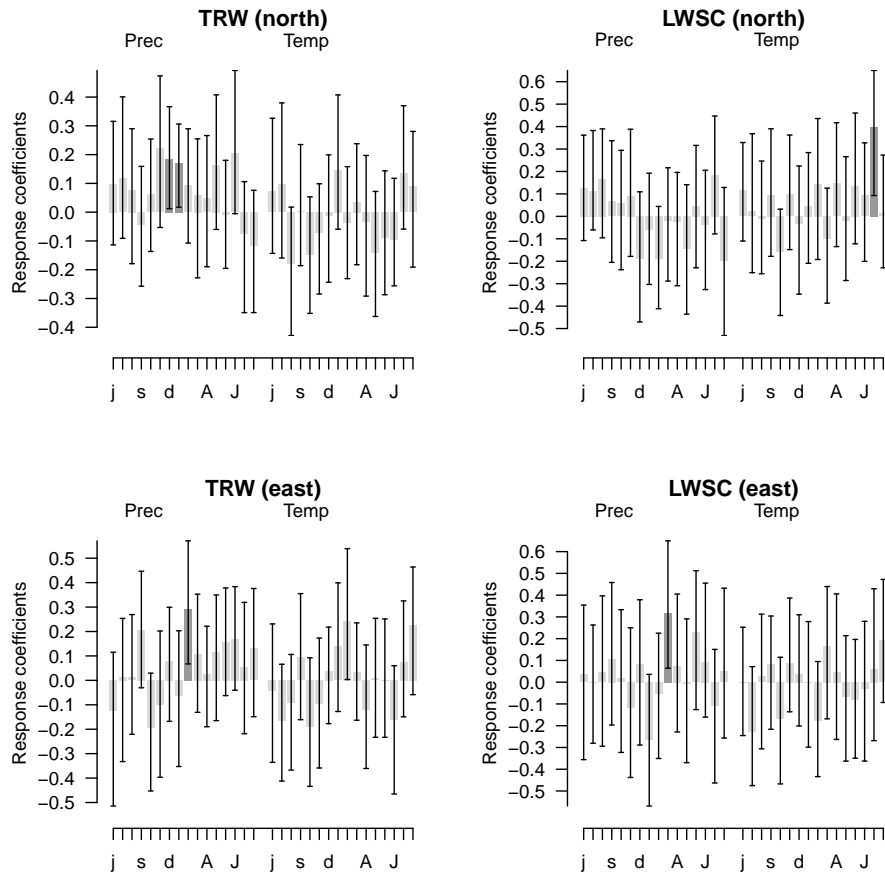


Figure 5: Intra-annual response coefficients for precipitation and temperature for Tree-ring Width (TRW) and Late-Wood Stable $\delta^{13}\text{C}$ (LWSC) chronologies of *P. pinaster*. The darker bars indicate significant coefficients ($P \leq 0.05$), and the lines represent 95%-confidence intervals.

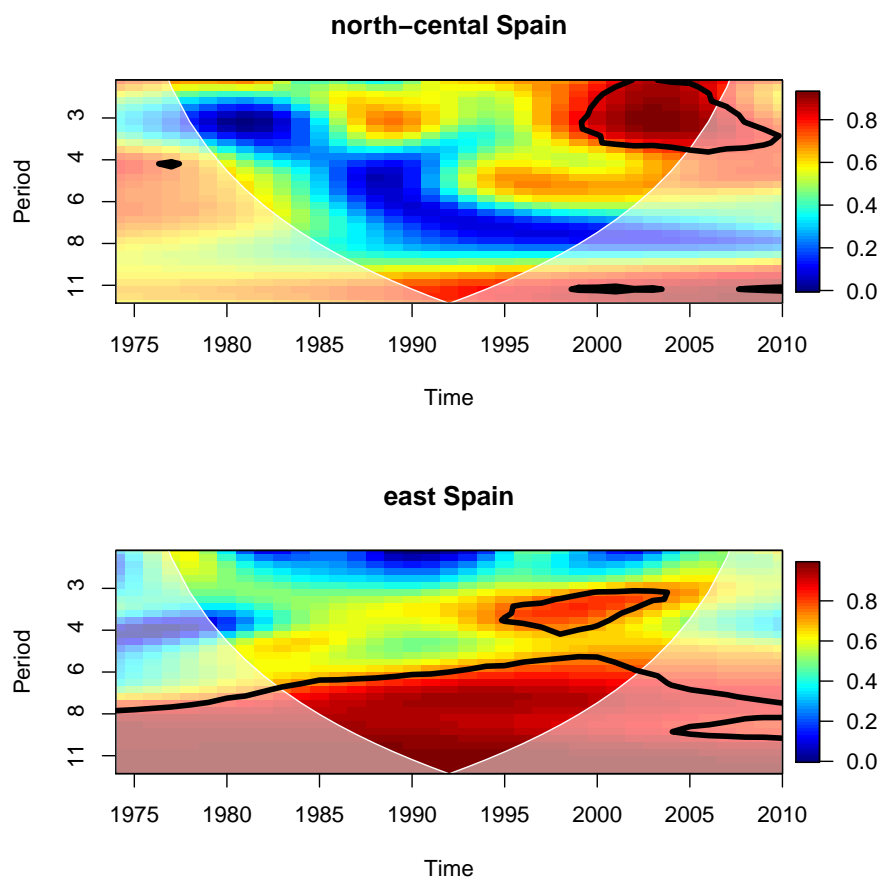


Figure 6: Wavelet coherency between signals of tree-ring widths and standardized precipitation indexes. The colored scale indicate the correlation between the two time series.